Available online at www.sciencedirect.com
SCIENCE DIRECT
International Journal of Heat and Mass Transfer 49 (2006) 1773–1789
International Journal of HEAT and MASS TRANSFER
www.elsevier.com/locate/ijhmt

Recommendations and guidelines for the performance of accurate heat transfer measurements in rapid forming processes

G. Dour [a,*], M. Dargusch [b], C. Davidson [c]

[a] CROMeP—Ecole des Mines d'Albi-Carmaux, Route de Teillet, 81 013 Albi Cedex 09, France
[b] Division of Materials, School of Engineering, CRC for Cast Metals Manufacturing (CAST), The University of Queensland, St. Lucia, Brisbane, QLD 4072, Australia
[c] CSIRO Manufacturing and Infrastructure Technology, CRC for Cast Metals Manufacturing (CAST), Pinjarra Hills 4069, Australia

Received 21 July 2005; received in revised form 10 October 2005
Available online 30 January 2006

Abstract

The published requirements for accurate measurement of heat transfer at the interface between two bodies have been reviewed. A strategy for reliable measurement has been established, based on the depth of the temperature sensors in the medium, on the inverse method parameters and on the time response of the sensors. Sources of both deterministic and stochastic errors have been investigated and a method to evaluate them has been proposed, with the help of a normalisation technique. The key normalisation variables are the duration of the heat input and the maximum heat flux density. An example of application of this technique in the field of high pressure die casting is demonstrated. The normalisation study, coupled with previous determination of the heat input duration, makes it possible to determine the optimum location for the sensors, along with an acceptable sampling rate and the thermocouples critical response-time (as well as eventual filter characteristics). Results from the gauge are used to assess the suitability of the initial design choices. In particular the unavoidable response time of the thermocouples is estimated by comparison with the normalised simulation.

1. Introduction

Heat transfer at the interface between two surfaces is a key parameter that controls many industrial processes, such as high loading or high speed wear, casting, forging, etc. In casting, heat transfer is particularly important because it controls the production rate and the microstructure of the products. Generally, mechanical properties improve with increasing solidification rate, although controlling the sequence of solidification from one part of the casting to another can be more important. With sand casting, the heat extraction rate is limited mainly by the poor thermal conductivity of the sand; the interface is of secondary importance. However in castings made in metal dies, the limiting factor is generally the casting-die interface. That is the reason why heat transfer coefficient has been studied for such a long time in various processes such as gravity die casting [1–5], low pressure die casting, high pressure die casting (HPDC) [4,6–12] and the more recent casting processes such as thixo or rheo-casting and squeeze casting. Less classical are the investigations of Inoue et al. [13] and Konovalov et al. [14] on the formation of metallic glass with the HPDC technique. In addition, heat transfer phenomena at a melt-metal interface have been extensively studied in strip casting because it appears to be one of the most limiting factors in the development of this technology [15–19].

However different casting processes can have very different interface characteristics. In gravity and low pressure die casting, the die is usually coated with a semipermanent thick (several hundred μm) layer of silicate-bonded refractory particles, such as talc, alumina, rutile or carbon. In processes involving higher pressures a "lubricant" or die-release agent is applied prior to each casting. In HPDC this

* Corresponding author. Tel.: +33 (0)5 6349 3165; fax: +33 (0)5 6349 3242.
E-mail address: dourdour@enstimac.fr (G. Dour).

0017-9310/$ - see front matter © 2006 Elsevier Ltd. All rights reserved.
doi:10.1016/j.ijheatmasstransfer.2005.10.045

Nomenclature

A	surface area
b	thermal effusivity
Bi	Biot number
C_p	specific heat capacity
$dt = 1/f$	time step of the sampling data
e, e^+	position of the closest thermocouple to the interface and same in normalised variables
f	sampling rate
Fo	Fourier number
h, h_c, h_{fl}, h_{fl}^+	heat transfer coefficient (or thermal conductance) of the interface, between a thermocouple and its solid surrounding, with a cooling fluid, same but in normalised variable
k	thermal conductivity
L, L_C, L_{sh}, L_{MgO}, L_{wire}	optimal and critical length of the fin (thermocouple penetration) and the contribution from the shield layer, of the insulator layer and of the thermocouples wire
m, m_E	inverse of a characteristic length of a fin inserted in a solid, same applied with the air as environment
ntf	number of future instant (used in our inverse method)
r	radius of a thermocouple
R	thermal resistance of the interface
R_a	roughness parameter; arithmetic roughness
r_C	resistance due to the finite contact between the gauge and the part
r_E	heat resistance between the gauge and the external environment
r_m	constriction resistance due to the gauge
s	Laplace transform variable
S_{i+k}^+	sensitivity coefficient at the time $i+k$ and is determined with functions in the Laplace space
t, t^+	time and normalised time
T, T^+, T_1, T_2, T_{sensor}, T_E, T_0	temperatures: of a piece of material; normalised; of the surface of side 1; of the surface of side 2; as given by a temperature sensor; of the environment, at $x = 0$ (the interface between die and external environment)
T_{i+k}^+, $T_{i+k}^+(\phi_i^+)$	input (measured or resulting from a numerical simulation in the present paper) temperature at location e+ and at the future instant $i+k$ passed time t (increment i) and temperature evaluated, at the same time and same location, with a numerical method (here thermal quadrupoles) and with the assumption that the heat flux density ϕ_i^+ remains constant during the future instants
T_{fl}, T_{fl}^+	temperature of the thermal regulation fluid, same normalised
V	volume
W_t	roughness parameters; undulation
x	axis parallel to the interface and to the thermocouples in the gauge
z, z^+	axis and distance perpendicular to the interface, normalised distance
κ	thermal diffusivity
ϕ, ϕ_{max}, ϕ_{exp}, ϕ^+, $d\phi^+$	heat flux density, maximum heat flux density of the heat input at the surface of the die, same as determined from experimental measurement and application of the IM, the normalised heat flux density and its increment from one time step to the next one
ρ	density
τ	duration of the heat input at the surface of the die
τ_{TC}, τ_{TC}	time response of a thermocouple
θ, $Y\theta$	Laplace transform of the temperature, and of the temperature of a sensor with a given time response

coating may be only a few nanometres thick [20]. In the first cases, the interface is a significant thermal barrier. Many studies have been conducted on the heat transfer through the coatings in foundry applications [1,3–7,21–23]. They all show that contact conditions change radically during the solidification and the cooling of the casting. At the very beginning of the casting the contact is a solid/liquid contact; then solidification takes place at the surface, leading to a solid/solid contact. Contraction of the solid takes place leading to the formation and growth of an air gap between the casting and the die (or its coating). The heat transfer is then limited by the radiation and the conduction through the air layer. Quoted heat transfer coefficients typically range from several thousand $W\,m^{-2}\,K^{-1}$ when the casting is liquid, dropping by up to an order of magnitude as it cools. Conduction through the coating is generally not treated separately, but lumped into an effective heat transfer coefficient. In high pressure die casting the situation is somewhat different. The die surface in contact with the melt is often polished, so surface roughness is less important. The die-spray helps to stop the melt from wetting the die, which would otherwise lead to close to perfect thermal contact. At a time between a few tens to a few hundreds of milliseconds after filling, a high pressure is applied, which forces the melt into close conformity with the die surface. This causes a substantial decrease in thermal resistance, probably limited by: surface tension and nonconformity against surface roughness; the finite thicknesses of layers with lower thermal conductivity (the mould and melt oxides and the organic die spray and/or its

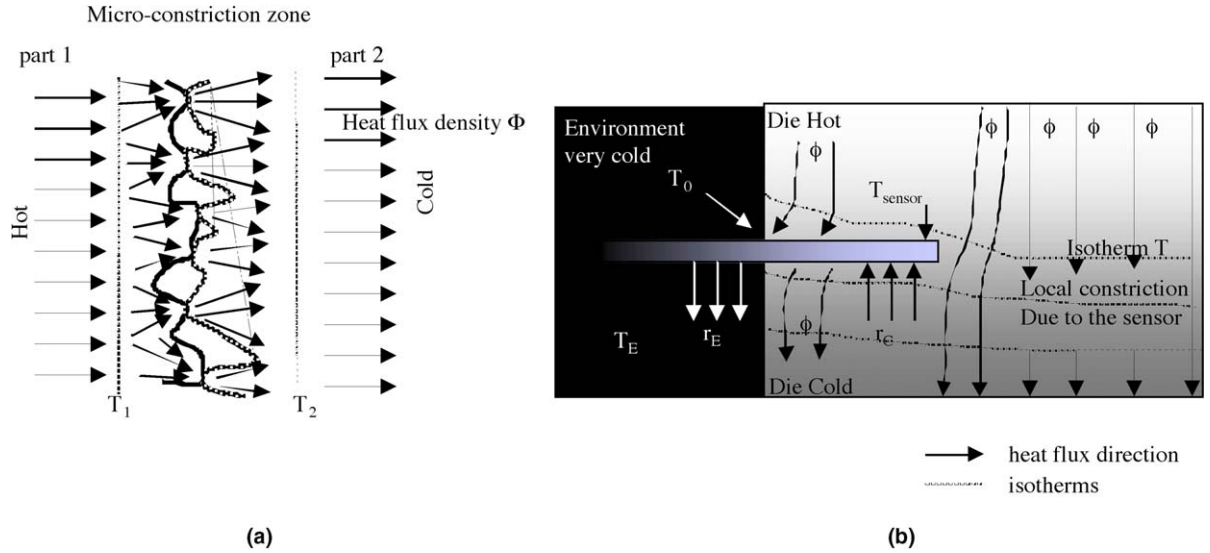

Fig. 1. Schematisation of (a) imperfect contact and the local constriction, (b) constriction due to the presence of a sensor and fin effect of a sensor. The direction of flux lines will vary according to relative contributions from fin effect and imperfect contact between thermocouple and mould.

thermal decomposition products). Nevertheless, very high heat fluxes are involved and these pose the most difficult experimental conditions of any casting process.

The usual method of modelling the heat transfer through the interface consists of: looking at the contact from a distance (about 10 times the surface roughness, see Fig. 1a) and considering that temperature is discontinuous from material 1 to material 2 and that the temperature drop in the gap and the interfacial films is controlled by the heat transferred between 1 and 2 and by an effective thermal contact resistance (TCR). The TCR, R, is then defined as the inverse of a heat transfer coefficient (or thermal conductance) h:

$$\Phi = h(T_1 - T_2) \quad (1)$$

$$R = 1/h \quad (2)$$

From a practical point of view, a single effective TCR can be applied, provided the heat capacity of the interface is negligible. This permits us to neglect the various heat transfer mechanisms that operate at the interface and determine a single empirical value. The evaluation of this parameter is classically performed with measurements of temperatures in the die and in the casting. The experimental results are then either compared to numerical simulation results with fitted interfacial parameters or exploited with an inverse model of the transient heat transfer. In all cases, the temperature measurements are converted into a heat flux density and transformed in a heat resistance through Eqs. (1) and (2).

The present paper will summarize the published work on measurement of temperatures and evaluation of interfacial heat transfer with the use of inverse methods. It does not discuss on the numerical treatment of the modelling, although the reader can refer to [24,1] where the thermal quadrupole method [25] and the Beck iterative method for the inverse modelling that we used are described. We then propose an experimental design methodology for construction of sensors suitable to a HPDC environment and a measurement strategy that permits reliable inverse modelling. The strategy is based on a normalisation technique used to summarize the problem. The same normalisation enables us to evaluate stochastic and deterministic errors in the heat flux determination. Finally results and analysis from HPDC trials are used to demonstrate the capability of the strategy.

2. Literature review about the difficulties in interfacial heat transfer determination

A number of precautions must be taken to ensure accurate results when measuring temperatures and evaluating the thermal properties of an interface. The following paragraphs summarize what can be found in the literature about these factors.

2.1. Perturbations due to the sensor location

These perturbations occur because any intrusive sensor will almost invariably modify the thermal field on a local scale, in both transient and steady state conditions. The sensor (in this case a thermocouple) is meant to give the temperature of the bulk of the die, not too far from the interface. Nevertheless it gives its own temperature and one hopes it is close to the temperature of the bulk. Reality can be very different if no care is taken.

The distortion of the thermal field by a thermocouple in a hole has been known for a long time. For example, Beck and Hurwicz [26] have analysed results under the steady state conditions of the limiting case of an empty hole parallel to the heat flow direction. The limit is equivalent to a

thermocouple with conductivity much lower than the die material. In this condition the die develops a hot-spot on the thermocouple axis, and under some conditions the temperature at the bottom of the hole (thermocouple measurement point) can even be higher than at the surface in a region unperturbed by the hole. The perturbation due to the presence of the hole increases with increasing the ratio of the hole radius to the thickness of the die between the hole and the surface. The error decreases as the thermocouple thermo-physical properties approach those of the die material and the contact resistance approaches zero.

Errors due to heat loss along a thermocouple have been most closely studied when the thermocouple is just contacting the surface and otherwise exposed to an external environment [27]. Of the parameters that are subject to some range of control, errors are found to increase with increasing wire radius or increasing thermal resistance between the wire and the die surface.

Placing the thermocouple in a hole parallel to the isotherms (normal to the heat flow direction) causes much less disturbance to the temperature field, but is more difficult to implement in practice. Attia et al. [28] have recently studied the steady state errors in this configuration. If the hole is deep enough (they used 10 times radius) and heat loss down the thermocouple wire is not significant then there is no systematic error if the thermocouple is positioned on the centreline of the hole. If the thermocouple is contacting the end of the hole eccentrically, and closer to the hot or cold side of the die, then there is an extra source of error. However the largest component of this error (about 80%) is simply due to the offset in the gradient, while the smaller fraction is due to the extra distortion from the presence of the thermocouple. In an attempt to summarize the wire, the distortion and the environment effect, Bardon et al. [29,30] proposed Eq. (3). The error of temperature ($T - T_{\text{sensor}}$) at the measuring point is expressed by a fraction of the temperature between the local point and the temperature away from the bulk ($T - T_{\text{E}}$) as described in Fig. 1b.

$$T - T_{\text{sensor}} = \frac{1}{1 + \frac{r_{\text{E}}}{r_{\text{m}} + r_{\text{c}}}} (T - T_{\text{E}}) \tag{3}$$

The conclusions that can be drawn from these studies, in as much as they pertain to die casting conditions, are that very thin thermocouples and holes should be used (to minimize r_{m}), with minimum thermal resistance at the medium/sensor contact (welding, brazing, stamping, etc.) to minimize r_{c}.

An alternate approach [31] is to have a thermocouple welded to the end of a hole parallel to the heat flow direction but with no packing around it and thus very poor contact with the wall. The presence of the hole can then be allowed for by being included in the inverse model. While this makes the model more complicated, it has an advantage of avoiding some of the uncertainty around important values such as r_{c}.

2.2. Influence of the sensor dynamic in transient experiments [32,33]

HPDC involves very rapid changes in die temperature and accurate response to transients is essential. Thermocouples are well known to have a slow response time that can drastically impair the accuracy of their measurements for fast transient heat transfer regimes. It is one reason why all authors agree on the fact that thermocouples must be as thin as possible and their contact with the sample as good as possible (i.e. low resistance r_{c}). A good approximation, appropriate to a step change in temperature, is usually given by the following set of equations ([33,34] for instance):

$$\rho C_{\text{p}} V \frac{\mathrm{d}T_{\text{sensor}}}{\mathrm{d}t} = h_{\text{c}} A (T - T_{\text{sensor}}) \tag{4}$$

where T_{sensor} is the temperature given by the sensor

T is the actual temperature to be measured
$h_{\text{c}} = 1/r_{\text{c}}$ is the conductance (or heat transfer coefficient) between the sensor and the specimen
V is the volume of the hot junction
A is the surface area at the contact zone
ρC_{p} is the volumetric heat capacity of the hot junction material

Therefore the response time τ_{TC} is given by Eq. (5). It is expressed in two ways, where the second, simplified, form applies to wires, ignoring end-effects:

$$\tau_{\text{TC}} = \frac{\rho C_{\text{p}} V}{h_{\text{c}} A} \tag{5}$$

Eq. (4) is only valid under a certain set of assumptions: the thermocouple is perfectly isolated from the environment (i.e. r_{E} is infinite) and radial thermal gradients in the thermocouple can be ignored (i.e., $Bi \ll 1$). The relevant parameter for thermocouples in conditions of high transfer is the intrinsic response time, the time to reach 63% of the final temperature when suddenly immersed in a perfect heat source at constant temperature. Nevertheless the response time more often refers to a standard test such as a dip in boiling water at normal atmospheric pressure. Milano et al. [33], for example, used 0.5 mm sheathed mineral-insulated thermocouples with grounded junctions. The response time is given to be 25 ms in the conditions of a dip in hot water. Some data can be found in manufacturers' technical reference books. For example, the Thermocoax's document gives the intrinsic response time for 0.25 mm grounded thermocouples as 7 ms [35]. Omega's reference book suggests that any response times are multiplied by a nominal factor of 1.5 when ungrounded construction is used [36].

Because most of the time the dynamics of the mounted sensor is controlled by the contact quality, it is only when thermocouples are well-coupled to a high heat-diffusivity medium such as a metal die that they may approach

intrinsic response times. But in most experimental mounting in a bulky medium, the contact is not perfect and it affects the response time. Because there is no way to step up the temperature in the bulk of such a medium, there is no simple way to evaluate the response time. In the IM development of the present paper, a method to evaluate the sensor dynamic from measurements will be proposed and applied to the data from HPDC.

2.3. Troubleshooting with inverse modelling

Inverse methods (IM) are useful numerical tools to evaluate boundary information from bulk measurements in an ill-posed problem. Nevertheless as with any numerical tool, they work well in a restricted parameter range. The width of the correct evaluation window depends on the numerical method that is used (FEM, DF, etc.) and on the method itself (sequential or function specification after Beck's principle, B-spline function, iterative regularisation, control theory such as Marquard, etc.) [37]. It is not the topic of the present paper to compare the different methods. Our objective is rather to find correct measurement strategy in order to be in the right window for the IM method of our choice [1,24]; Beck's principle and thermal quadrupoles [25] for the numerical tool. Outside the targeted window, instability has been reported, as well as inaccuracy. The latter find its origin in different sources listed in literature as deterministic or stochastic errors and also as linked to the sensors dynamic. Some of the requirements that are reported in the literature for a good estimation are summarised below.

Stability of the IM. IM have a tendency to be unstable. The factors that influence this instability are the depth, e, of the reference bulk thermal sensors, the sampling rate, f, of the data acquisition (or the time step of the data acquisition, $\mathrm{d}t$) and the thermal diffusivity of the materials, κ [38,39]. According to those authors, the following Fourier number characterises the tendency to stability:

$$Fo = \frac{\kappa\,\mathrm{d}t}{e^2} \tag{6}$$

The Fourier number Fo should be between 1 and 0.01 to obtain a reliable resolution of the problem. When it is between 0.001 and 0.01 the resolution may be unstable depending of the Signal/Noise ratio and filtering techniques can be employed to solve the problem. Below 0.001, the IM will be unstable whatever temperature input (even taken from an analytical expression).

Deterministic error. This refers to the error in the interfacial heat exchange determination due to inaccuracies in the chain of measurements: the accuracy of the temperature measurement; the accuracy of the thermocouple location; and the accuracy of the thermal property data. Some authors [40–42] have worked on optimising the experiments in order to minimise the impact of those inaccuracies. The strategy they advise is to locate the sensor as close to the surface as possible, to reduce the sampling rate and to use a large dimension for the B-spline extrapolation (or equivalently the number of future instants, ntf).

Stochastic error. Stochastic errors correspond to the errors introduced by any small variation in the temperature measurements, such as noise. These errors have been investigated by Flach and Özisik [43] for instance who state that the best strategy to reduce them is to decrease the time step, reduce sensor depth from the surface and increase the B-spline dimension. Note that the time step requirement conflicts with optimising the deterministic error.

Effect of the thermocouple response time. Woodbury [32] has studied the impact of the response time of thermocouples on the heat flux density prediction. It appears that the heat flux density estimation lags by an amount of the order of magnitude of the time response of the sensor and it can be seriously underestimated depending on the response time. Significant errors develop if the sensor response time is one tenth of that of the heat input event being determined, and errors get larger if the sensor has a longer response time.

2.4. Conclusion of the literature review

As a conclusion of our bibliography analysis, the instrumentation to determine the temperature input required in an inverse method used for a surface or interface heat flux determination has to respect a number of rules:

- Accurate temperature measurements in a metallic die require a very good contact between the sensor and the bulk metal along its isothermal surfaces.
- The sensors should be as thin as possible, to minimise the perturbation to heat flow and to have the short response times essential for accurate measurement under rapid transient heat transfer conditions.
- The first thermocouple must be as close as possible to the surface to minimise both deterministic and stochastic inaccuracies. The limit to this will usually be determined by practical difficulties (proximity to the surface). As the distance from the surface approaches the dimension of the thermocouple, the distortion of the thermal field increases, leading to other errors.
- The time step for the measurement must be chosen as a compromise between the amplification of stochastic errors and the propagation of deterministic errors.

Our personal understanding of the literature is that a hidden parameter is hardly mentioned but is always present in all the investigations. The IM analysis is made necessary because the transfer under consideration is transient. To us the hidden parameter in this "short time problem" is the duration of the heat input. What makes the comparison between one paper and another difficult is that the durations of the heat input are rarely similar. As a matter of fact, the optimum time step, $\mathrm{d}t$, the position of the first sensor, e, (as used in the Fourier expression Eq. (6)) and the impact of the sensors response time τ_{TC} are all determined

by the duration of the heat input. The situation will be completely different if the observed phenomena last 0.1 s or 1 min. A given sensor dynamic (say 50 ms) would be of crucial importance in the first case and could be ignored in the latter. The time step of data logging (say 50 Hz) would be largely enough to describe the thermal phenomena in the second case but hardly sufficient for the former. In our analysis, the thermal input duration plays a major role as can be read in the following.

3. A strategy to minimise the effect of environment on thermocouple measurements

When one intends to measure the temperature in the bulk of a material subjected to high temperature gradients, it is necessary for the sensor to lay along the temperature isotherms. Otherwise heat can flow along the sensor, which has different thermal properties from the bulk materials. This would result in modification of the local heat balance and inaccuracy of the temperature measurement (the temperature reported by the sensor is then not equal to the temperature that would have been at that point in the original material) [29].

Because thermocouples are wire type sensors, part of the wire will lay in gradient zones and be in contact with the environment that is at a different temperature. It is important to make sure that it does not concern the tip of the thermocouple (that must lie along an isothermal line) and that the hot junction is not influenced by it (gradient zone must be far enough from the tip). When a long, thin cylinder (radius r) is set in contact with a medium with a constant temperature T along its large dimension and set at an imposed temperature T_0 at the edge ($x = 0$), the temperature profile $T_{\text{sensor}}(x)$ follows a classical equation (7), provided that the Biot number $Bi = h_c r/k$ is small compared to 1. This problem is similar to the thermal fin concept [44] lying in a fluid at uniform mixing temperature exchanging heat with the fin through a boundary layer characterised by a heat transfer coefficient; here h_c is rigorously a thermal conductance, but because the medium is at a uniform temperature (along an isothermal line or surface) it can be considered equally as a heat transfer coefficient [45]. The solution is then Eq. (8).

$$\frac{d^2 T_{\text{sensor}}}{dx^2} - \frac{2h_c}{kr}(T_{\text{sensor}} - T) = 0 \tag{7}$$

$$T_{\text{sensor}}(x) - T = (T_0 - T)\exp(-mx) \tag{8}$$

with

$$m = \sqrt{\frac{2h_c}{kr}} \tag{9}$$

The same equation holds if the thermocouple is extended into the external fluid environment ($x < 0$) at the mixing temperature T_E, but with a different value for the heat transfer coefficient. The value of T_0 is unknown in this scenario, but can be determined as follows. Conservation of energy requires that the thermal gradient has the same value in the limit as both equations approach $x = 0$. This equality leads to

$$T_0 = \frac{m_E T_E + mT}{m_E + m} \tag{10}$$

Singh et al. [46] have given a more detailed solution including the end-effects, which reduces to Eq. (10) when end-effects are insignificant.

In HPDC conditions that we chose for an application field (see below), the die temperature usually lies around 200 °C and room temperature is about 20 °C. An absolute error of 10 °C on the thermocouple measurements corresponds to 5% of $(T - T_E)$. In order to keep the error in that 10 °C range, the length of the fin must respect Eq. (11).

$$L \geqslant \frac{1}{m}\ln\left[20\frac{m_E}{m + m_E}\right] \tag{11}$$

In the occurrence of $m_E = m$, the expression becomes

$$L_c = \frac{2.3}{m} \quad \text{(expressed in meters)} \tag{12}$$

Eqs. (11) and (12) have been used to do some numerical application with the most conductive material in a K-type thermocouple (alumel). The air heat transfer coefficient has been varied from still air condition to stirred air conditions (h from 5 to 200 W m^{-2} K^{-1} after [47]), the thermal conductance h_c was taken to be 1000 W m^{-2} K^{-1} corresponding to a poor contact conduction after [48] and the radius is taken to be 0.5 mm. Table 1 reports the different values of m, m_E and of the expression Eqs. (11) and (12). Because m_E is much lower than m, the length L appears much lower than L_C. It is only for the highest values of h_E and m_E that L tends to L_C. In most conditions, the exact value of m_E is not known and is difficult to find out, but is likely to be much less than m. In order to get a small error, we will use Eq. (12) as a limiting case in the discussion below.

The above equations apply to homogeneous fin material, but a sheathed thermocouple is made of several layers of different materials. The following analysis is one approach to account for the heterogeneous structure of a sheathed insulated thermocouple with a grounded hot junction. The thermocouple can be considered as a combination of three fins (as illustrated in Fig. 2):

1. the sheath, surrounded by the isothermal slab at T.
2. the insulating layer surrounded by the sheath once it is isothermal at T (within ΔT).

Table 1
Numerical application of Eq. (11) and Eq. (12) for a 0.5 mm alumel rod placed along isothermal lines with $h_c = 1000$ W m^{-2} K^{-1} and different values of heat transfer coefficient in the air

m (m^{-1})	m_E (m^{-1})	L (m)	L_C (m)	h_E (W m^{-2} K^{-1})
111.8	7.9	0.002	0.021	5
111.8	15.8	0.008	0.021	20
111.8	25.0	0.012	0.021	50
111.8	35.3	0.014	0.021	100
111.8	50.0	0.016	0.021	200

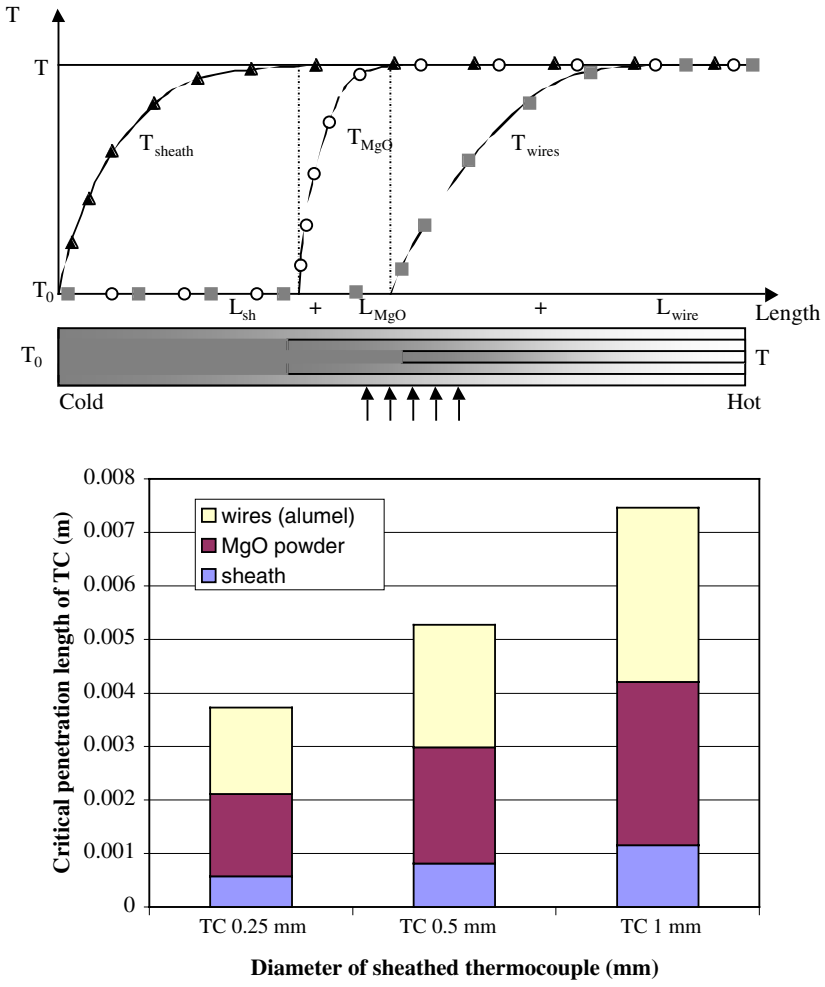

Fig. 2. Length of penetration for different diameter of sheathed insulated thermocouples (data is taken from Table 1 as justified in the text).

3. the thermocouple wires (treated as a single average material) surrounded by the insulating layer once it reaches $T - \Delta T$.

An over-dimensioning rule suggests that each fin should be dimensioned with respect to Eq. (12) giving three lengths L_{sh}, L_{MgO}, L_{wire}. To make sure that the thermocouple indication corresponds to its surroundings bulk temperature, a length L of the thermocouple should be inserted into the bulk according to the relation

$$L = L_{sh} + L_{MgO} + L_{wire} \tag{13}$$

To do a numerical application of the penetration length Eq. (13), we use the size data reported by Milano [33] and homothetic relations for new sizes (1 mm and 0.25 mm TC) and the thermo-physical property assumptions given in Table 2. The thermo-physical values of Table 2 are justified in the note at the end of the paper. The Biot number, Bi, of each layer of the thermocouple is evaluated: it is always lower than 1, which justifies the use of Eq. (7). From these data, we obtain the histograms of Fig. 2.

In our practical HPDC application, a die insert of 12 mm diameter we instrumented with three pairs of thermocouples at different position for the mating face. The thermocouples from the same pair are facing each other. In order to avoid interference between each of them, we had to use 0.25 mm thermocouples inserted a length of 4 mm along a radius.

Table 2
Physical and transfer properties used in Fig. 2

	Sheath	MgO	Wires (alumel)
Conductivity ($W\,m^{-1}\,K^{-1}$)	15	10	32
Heat transfer coefficient [a] ($W\,m^{-2}\,K^{-1}$)	10000	1000	1000
Biot number for the 0.25 mm TC	0.08	0.017	0.002
Biot number for the 0.5 mm TC	0.17	0.035	0.004
Biot number for the 1 mm TC	0.33	0.07	0.002

[a] The heat transfer coefficient are estimated coefficient according to our personal experience and readings such as [29,30,47,58,59].

4. An instrumentation strategy to make the Inverse Modelling (IM) relevant

As seen from the bibliography review, IM does not always give reasonable results. If the measurement strategy

is not correct, the method can be unstable or simply give an inaccurate evaluation of the heat flux density (which is our interest). The time response of the thermocouples can also have an impact on the relevance of the IM estimation. We aim here at describing the strategy we adopted to make sure our instrumentation always lead to good conditions for the IM to work and give accurate results. The strategy is based on a normalised analysis of the heat transfer problem. The principal variable of the normalisation is chosen to be the duration of the heat input in our transient casting problem. The normalised approach enables handling all the variables into a few normalised groups of them, which considerably simplifies the analysis. Following the literature classification of troubleshooting with IM, we then describe separately the deterministic errors and the stochastic errors. The impact of the time response of sensors can be handled as well as it is shown in the last paragraph of this section.

4.1. Normalisation of the thermal problem

As traditionally taught (e.g., [47]), heat transfer problems can be normalised using variables such as a reference temperature, a reference distance and the thermal properties of the materials involved. In most of the published studies on IM and some previous studies by the authors [49], another set of variables was used: the maximum heat flux density, a reference distance (either the position of the first thermocouple or the thickness of the slab) and the thermal properties of the materials. The choice of variables mostly depends on the analysis that is aimed at. This versatility is the great advantage of normalisation techniques.

According to our literature understanding, the duration of the heat input is the key parameter in transient heat transfer problem that should determine what strategy to adopt for the instrumentation. For the normalisation of a transient problem we obviously choose a set of parameters including the heat input duration plus some other parameters inspired from [49]:

- the heat input duration, τ
- the maximum heat flux density, $\phi_{\max}$
- the thermal properties of the materials, k and κ

The set of variables and equations are then normalised in the following way:

$$t^+ = \frac{t}{\tau}, \quad z^+ = \frac{z}{\sqrt{\kappa\tau}}, \quad \phi^+(t^+) = \frac{\phi(t)}{\phi_{\max}}$$

and (14)

$$T^+(z^+, t^+) = \frac{T(z,t)K}{\phi_{\max}\sqrt{\kappa\tau}} = \frac{T(z,t)b}{\phi_{\max}\sqrt{\tau}}$$

where κ is the thermal diffusivity

$$b = \frac{k}{\sqrt{\kappa}} \text{ is the thermal effusivity} \quad (15)$$

The heat conduction equation is transformed into

$$\frac{\partial^2 T^+}{\partial z^{+2}} - \frac{\partial T^+}{\partial t^+} = 0 \quad (16)$$

The initial condition is $T(t=0, z) = 0$, which transforms into $T^+(t^+ = 0, z^+) = 0$, and the boundary conditions are:

- on the mating surface

$$\phi(t) = -K\frac{\partial T}{\partial z} \text{ is transformed into } \phi^+(t^+) = -\frac{\partial T^+}{\partial z^+} \quad (17)$$

- on the rear surface

$$h_{fl}\left(T(t, z_{\text{rear}}) - T_{fl}\right) = -k\frac{\partial T}{\partial z} \text{ is transformed into}$$

$$h_{fl}^+\left(T^+(t^+, z_{\text{rear}}^+) - T_{fl}^+\right) = -\frac{\partial T^+}{\partial z^+} \quad (18)$$

$$\text{with } h_{fl}^+ = \frac{h_{fl}\sqrt{\kappa\tau}}{k} = \frac{h_{fl}\sqrt{\tau}}{b} \quad (19)$$

The rear surface is modelled as being in contact with a coolant of fixed temperature T_{fl} (or T_{fl}^+). This also defines the starting temperature of the material.

As a conclusion, the normalised problem is equivalent to a thermal conduction problem in a material with a thermal conductivity equal to 1 and diffusivity equal to 1. The initial temperature is here set to 0 everywhere in the slab. The maximum heat flux density applied on the hot surface is 1 and lasts 1 normalised time. The rear boundary condition is characterised by a heat transfer coefficient that may take any value and a coolant fluid whose temperature is here set to 0.

4.2. The strategy for the choice of the inverse method parameters

An evaluation of the temperature field has been done in the normalised conditions using the thermal quadrupoles direct method [25] (which is similar to an analytical solution but in the Laplace transform space), with a heat input in the form of a square function that lasts time $\tau^+ = 1$ with a maximum set to $\phi^+ = 1$. One example set of temperature curves vs. time and normalised depth in the slab is given in Fig. 3. Such a data is used as the temperature input necessary for the IM boundary condition evaluations. The IM that was used for that purpose is based on Beck's sequential method. At a time t (and index i), the increment of heat flux density, $\mathrm{d}\phi^+$, is evaluated with Eq. (20). The sensitivity coefficients S_{i+k}^+ are evaluated for the geometry of the problem. The input temperatures are T_{i+k}^+. The temperature $T_{i+k}^+(\phi_i^+)$ are, in fact, direct evaluation of temperature for the ntf future instants (from the time i to time $i + \text{ntf}$) when one makes the assumption that the heat flux density remains constant at the value ϕ_i^+ found at time i.

$$\mathrm{d}\phi^+ = \frac{\sum_{k=1}^{k=\text{ntf}} S_{i+k}^+\left[T_{i+k}^+ - T_{i+k}^+(\phi_i^+)\right]}{\sum_{k=1}^{k=\text{ntf}} S_{i+K}^{+2}} \quad (20)$$

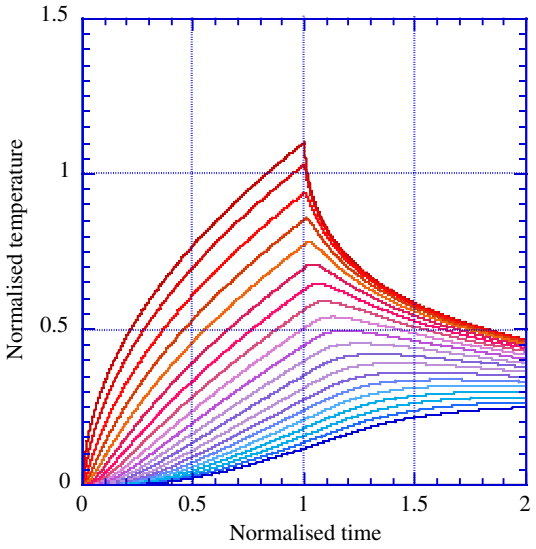

Fig. 3. Temperature curves used as a data for the IM to determine the map of relevance. The position relative to each temperature varies from depth 0 to the rear position with steps of normalised 0.1 distance (only the first the positions are shown).

The present IM is applied to the normalised heat conduction problem and under multiple conditions, using a range of sampling rates (or time increment from index i to $i+1$), a set of temperature inputs at a range of distances e^+ from the interface and a range of rear surface conditions (that may influence the input temperatures). Examples of the range of observed results are given in Fig. 4. The thick curves represent the evaluated heat flux density (to be compared to the square function used to get the temperature data) and the thin curves represent the error in the evaluation of the temperature at e^+ (position where the optimisation is performed). When the estimation is fine, the error curves remain small even at peak values, less than 0.01. An error larger than 0.1 is qualified unacceptable. Curves labelled "overestimation", "nonsense" and "unstable" give examples of fits that are deemed to be unacceptable. Depending on the attributed character, the heat flux density curves either show an overestimation of more than 10% than the reference value (set to 1), or may give a reasonable value but does not represent the square function at all or oscillates with amplitude larger than the reference 1. As can be seen from Fig. 4, even with a smooth input the IM may be fully unstable (bottom curves). The analysis of the stochastic errors will give a more precise definition of the stability for more realistic data (with noise).

Fig. 5 shows the derived map of relevance, where the quality attributes of the IM response to a smooth data are plotted as a function of the location e^+, the sampling rate, $\mathrm{d}t^+$ and the number of future instants, ntf. Four zones appear in the map:

Acceptable zone. In that zone the heat flux history is precise: the square function can be found easily and the step value is close to the expected 1 with an error less that 10%. A time response inherent from the inverse method itself or some damped oscillations may alter the response, but they last less than 0.2 normalised time. Estimations deemed "fair" to "very good" (see Fig. 4) are placed in the acceptable zone.

Unstable zone. In that area the inverse method is unstable (oscillations larger than 1). The results of the IM cannot be used because they have no relevance at all. It is possible to shift the boundary between acceptable and unstable by changing the number of future instants. With 10 future instants, one finds the Fourier parameter as described in [38] and reported in Eq. (6) for the limit between the stable and unstable zones.

Under or over estimation zone. In that zone, the time response of the measurement is so long that the heat flux density is not estimated properly. In some cases, the evaluation is overestimated and in others it is underestimated depending on the location of the rear data. The error does not exceed 20% in our numerical experiment, nevertheless such a zone should be avoided.

Nonsense zone. The square type of evolution is not found anymore, the derived heat input has little correlation with the imposed one. The result of the IM is consequently not relevant.

From this map, any reader realises that setting an experiment in order to perform IM calculation of heat flux density is greatly risky. If no care is taken, the chances are very thin to fall in the narrow acceptable zone. Most chance would be to find oneself in the unstable zone. Prior to any experiments for IM evaluation, extra care should be taken, especially in fast processes. The present map indicates that the preparation and design of sensor will depend on (1) the duration τ of the phenomena you want to study, (2) the position of the critical thermocouple, e. From these two, the data sampling rate, $\mathrm{d}t$, can be chosen so that you fall in the right area.

The dashed zone on the left end of the map has been set as a reminder that instrumentation should not be too close to the surface. It would be useless to locate a sensor (even a micro-sensor) in the first $10 * W_t$ or R_a of the surface, because the heat flux is constricted by the surface profile in this area.

The points noted 1–4 on the map of relevance Fig. 5 are the points that are recommended for an optimum IM determination. They are in the Acceptable Zone, with a high sampling rate (low $\mathrm{d}t$) enabling a doubling of the time step if necessary without falling in the Nonsense Zone. Care will have to be taken to avoid instability, and the number of future instants will have to be optimised, probably between 5 and 10. Point 5 is too close to the Under or Over estimation Zone to be reliable.

Point 3 will be chosen in our HPDC experimental study. Knowing that the duration of the phenomena to be observed is 0.5 s, we chose $e = 1$ mm and consequently $f = 200$ Hz.

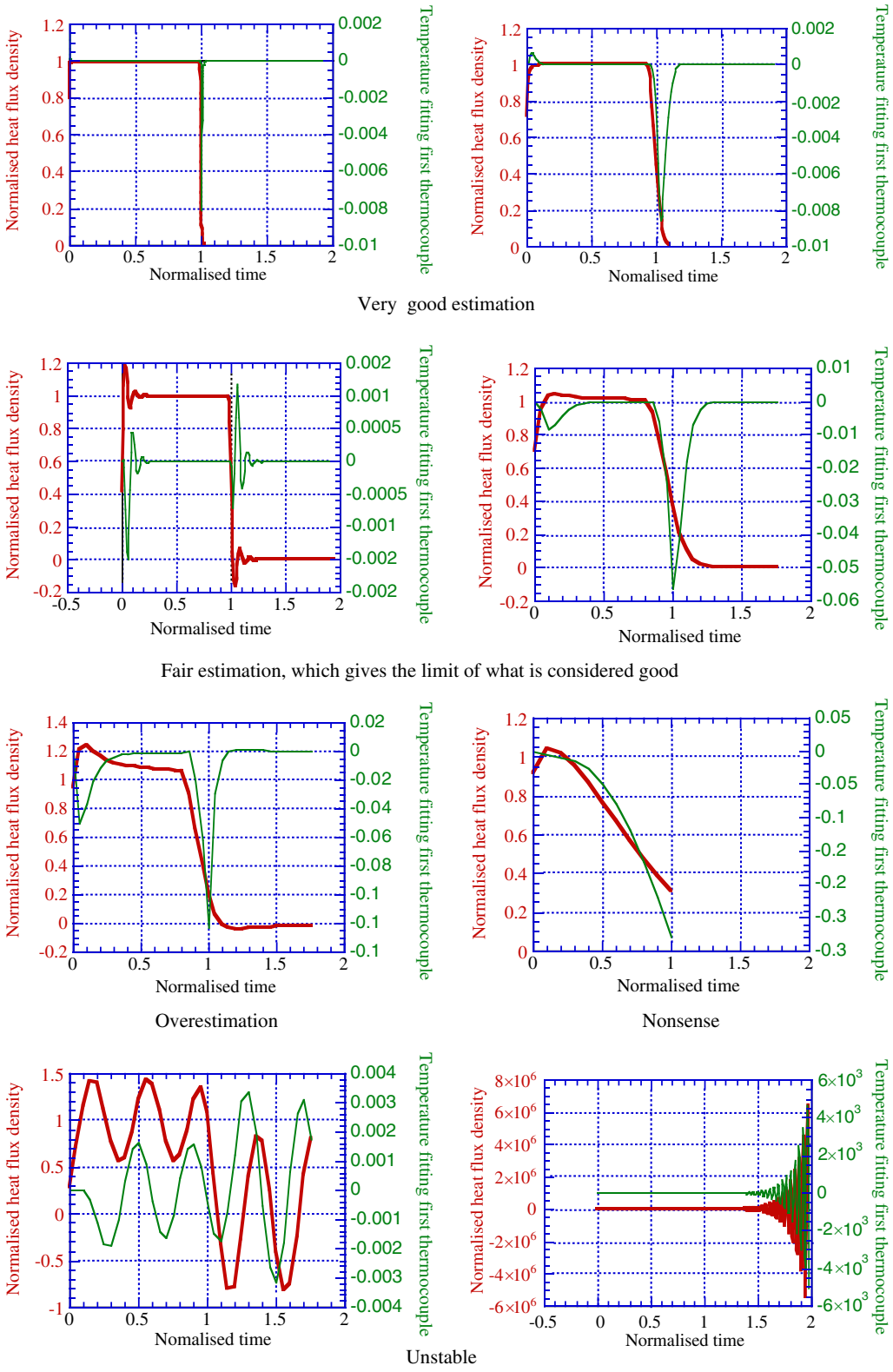

Fig. 4. Examples of the quality of results from the inverse method, taken under different sampling rates and measurement depths—Bold curves: evaluated heat flux density to be compared with a step function; Fine curves: residual error between the evaluated temperature and the data used at the closest position.

4.3. Evaluation of the stochastic errors

The stochastic error is the response of the method to some noise in the temperature data. A random noise was introduced to the simulated temperature readings (such as in Fig. 3). The amplitude is chosen to be 0.05, which is about 5% of the maximum temperature. The signal over noise ratio (S/N) is 20. The IM is applied using that noisy

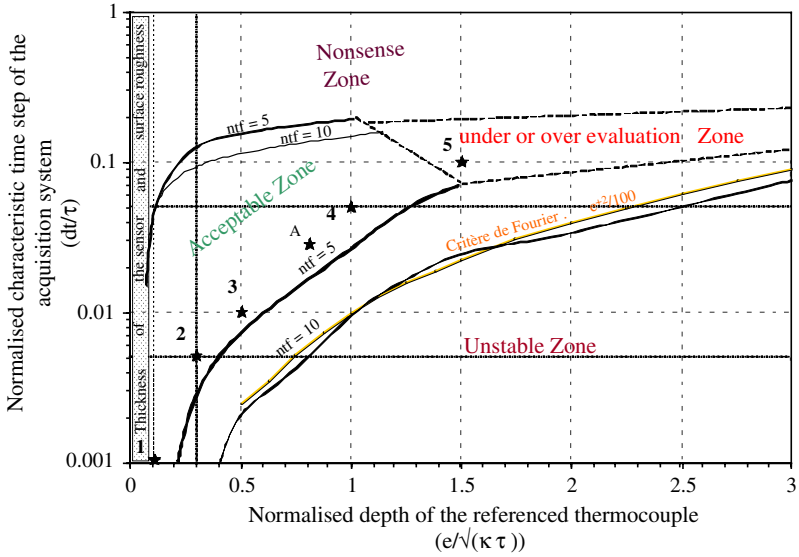

Fig. 5. Map of relevance of the inverse method for a smooth temperature.

data as an input. The two curves Fig. 6 report the heat flux density evaluation for point 3 of the map of relevance. With a smoothed data, the IM gives "very good" results with ntf = 5 and 10. It is clear for Fig. 6 that any noise strongly affects the response of the inverse method; a noise of 5% intensity can be amplified up to a noise of 200% intensity in terms of heat flux density. The impact of the number of future instants is demonstrated with the use of ntf = 5 and 10. Increasing the number of future instants drastically improves the estimation: with ntf = 5 the S/N

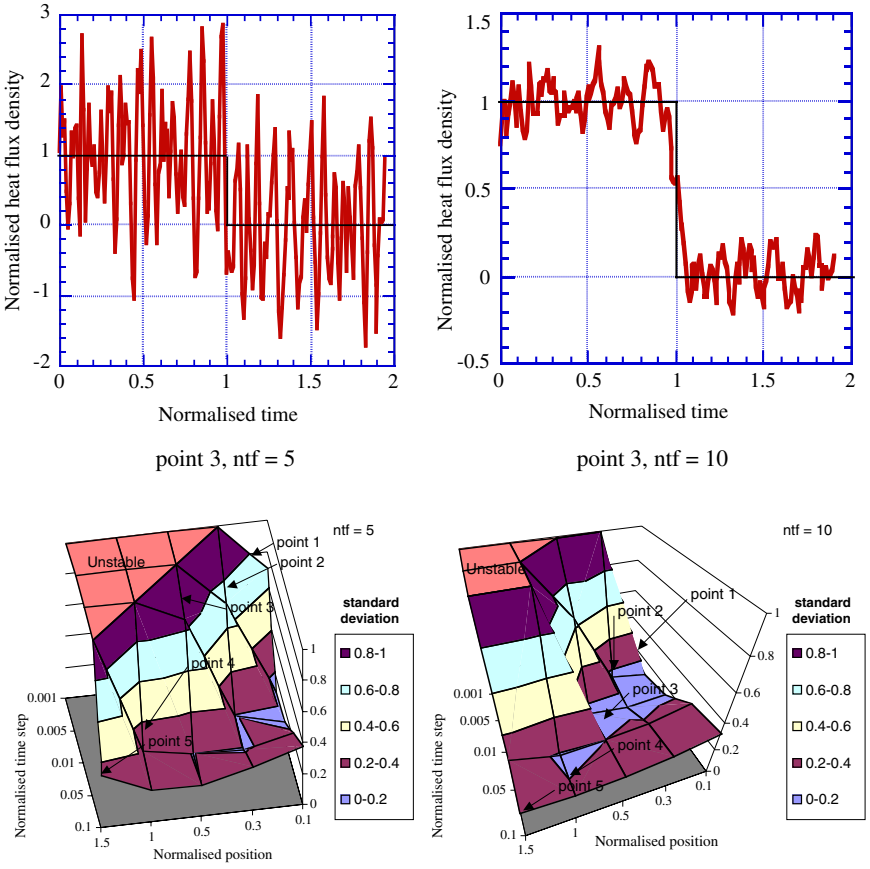

Fig. 6. Stochastic error of the IM with two choices of numbers of future instants (ntf), examples of data set for point 3 of the map of relevance and complete maps of the standard deviation vs. the normalised position and the normalised time step.

ratio is so small (about 0.5) that it is impossible to recognise any characteristics of the signal, whereas with ntf = 10 (S/N = 5) it is possible to find out the square characteristics of the original input. The 3D maps in Fig. 6 show the noise of the IM response in terms of heat flux density during the thermal input duration (1 normalised duration). During that period the perfect response should be constant equal to 1 without any noise. Consequently the standard deviation of the IM response during that period quantifies the stability of the IM relatively to noisy data. The maps have been saturated for large noise for the sake of visualisation: for all the values of standard deviation superior to 1 (for a signal that should be 1, i.e. S/N is 1), the IM has been considered unstable and classified in a "unstable zone". As for the map of relevance (Fig. 5), the "unstable zone" defined here is also reduced when a large ntf is used. The strategic points 1–5 have been positioned and the maps show that their associated standard deviations are more or less important depending on the value of ntf. As a matter of fact, point 4 should be preferred if the data were noisy and ntf had to be small. Position 1, 2 and 3 should be avoided with noisy data and low ntf. It is possible to push some them in a better position if ntf is increased up to 10. The discussion about best parameter sets to avoid unstability does not seem as obvious as it sounded in the literature. For instance, point 1 or 2 gave similar results to point 3 when ntf = 10, but better results with ntf = 5. This agrees with the conclusions of Flach and Özisik [43] about the interest of decreasing the time step, but the trend depicted in the maps indicates that decreasing time step (at constant depth) usually worsen the quality of the IM results.

As a matter of strategy to reduce the stochastic error, a noisy signal should be treated firstly in the IM by processing it with a large number of future instants. If this were to fail, the signal data could be shortened using a larger time step. One could be tempted to use a low-pass filter to smooth the input data. If ever this was to be performed, it is important to make sure that the filter's time response remains not more than 20% of the duration of the heat input (as it is discussed further with the effect of thermocouple kinetics).

4.4. Evaluation of the deterministic errors

Our normalised analysis enables a direct evaluation of the deterministic errors due to the inaccuracy of the physical properties and of the temperature measurements. From the derivation of Eq. (14), once τ has been chosen and T^+ has been evaluated from the charts such as Fig. 3, one can write that the error on ϕ_{max} is directly related to the inaccuracy of the temperature measurement and of the thermal properties of the die by Eq. (21).

$$\frac{d\phi_{max}}{\phi_{max}} = \frac{dT}{T} + \frac{db}{b} = \frac{dT}{T} + \frac{dk}{k} + \frac{1}{2}\frac{d\kappa}{\kappa} \tag{21}$$

Another source of error is the location of the reference thermocouple. If the temperature at two positions in the neighbourhood of the reference thermocouple ($e^+ \pm 0.1$) was measured and the inverse method was applied wrongly assuming these temperatures were taken at the position e^+, one would get the results shown in Fig. 7. If the location is 0.1 further than expected, the heat flux density increases slowly to a steady maximum value. If the location is 0.1 closer than expected, the heat flux density shows a very high but short time peak and then decreases slowly to a steady minimum value. In each case the final value is about 6–7% lower or higher than the expected value although the relative error in position is 33%. Another way to evaluate this impact could be to evaluate the temperature measurement error due to the position inaccuracy and then apply Eq. (21). The error of temperature measurement due to the location is related to the thermal gradients in the die, according to Eq. (22):

$$dT = T(z\,dz, t) - T(z, t) = \frac{dT}{dz}dz \approx -\frac{\phi_{max}}{k}dz \tag{22}$$

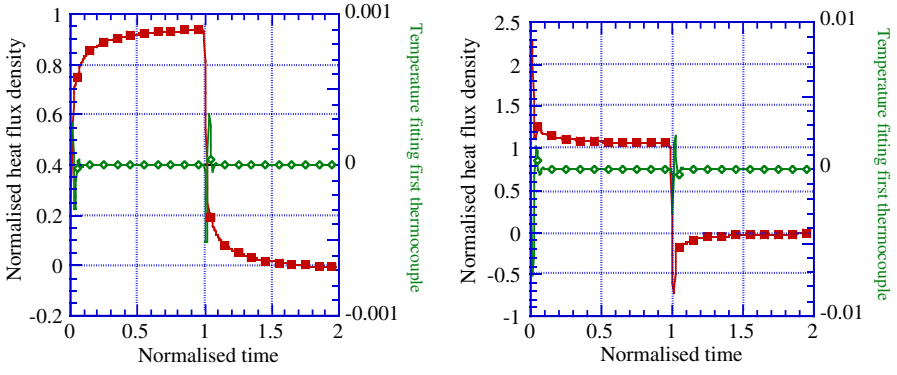

Fig. 7. Impact of the inaccuracy of the location of the reference thermocouple on the heat flux density evaluation (full square) and on the temperature error at the optimising point (open diamond).

Then the relative inaccuracy of the heat flux density estimation being equal to dT/T everything else being perfect (Eq. (21)), the error due to the location of the thermocouple writes as

$$\frac{d\phi_{max}}{\phi_{max}} = -\frac{\phi_{max}}{kT}dz \tag{23}$$

If applied to the normalised situation, the maximum heat flux density is set to 1, the thermal conductivity is set to 1 and the temperatures involved are around 1 for a duration of 1 (see Fig. 3), which leads to a relative error on the evaluation of the heat flux density from the error of the location. In the simulation that was performed above, one should find 10% inaccuracy, higher when $dz < 0$ and lower when $dz > 0$. The simulation gave 6–7% with the same signs.

As a matter of fact, the precision of our evaluation of heat flux density in the following HPDC experiment is determined by

- precision of temperature measurement, which the sum of (1) the precision of the sensors (±1.5 °C for class 1 thermocouples) and (2) the precision of the fin tip (estimated to 10 °C with expression (11));
- precision of the thermal properties of the tool steel (it is know with 10% accuracy according to the measurement company);
- precision of the position of the sensors (±0.03 mm according to the manufacturer) for $e = 1$ mm.

All in all, the relative precision applied with the maximum temperature (about 400 °C) and maximum value of heat flux density about (10 MW/m^2) is 15% for the evaluation of the heat flux density, provided that the IM is used in the acceptable zone.

4.5. Impact of sensors kinetics

We consider the sensor as a first order filter, with a time response τ_{TC}. Because of the normalisation approach that was used to locate the best position of the thermocouples, we normalise the time response of the filter with the same parameter, τ, the duration of the heat input. The time response τ_{TC} becomes $\tau^+_{TC} = \tau_{TC}/\tau$. The influence of τ^+_{TC} on the temperature measurement and consequently on the IM heat flux determination has been determined for four response times, namely 5%, 10%, 20% and 50% of the heat input duration. The investigation has been conducted as follows:

- evaluation of the Laplace transform of the temperature under conditions corresponding to points 1–5 on the map of relevance, following application of the standard heat input;
- evaluation of the delayed response from the thermocouples, using Eq. (24) applied to the Laplace transform of the temperature;

$$Y\theta(s,x) = \frac{1}{s\tau^+_{TC} + 1}\theta(s,x) \tag{24}$$

where

$\theta(s, x)$ is the temperature calculated from the thermal equation after Laplace transformation
s is the t-corresponding variable in the Laplace space
$Y\theta(s, x)$ is the temperature of a first order filter in the Laplace space

- application of the IM using the delayed responses as temperature data and reverse the Laplace transform using the standard method used with thermal quadrupoles [25].

Fig. 8 gives one example of results for the strategic point 3 of Fig. 5. On the left set of curves, the temperature at point e^+ is given as a function of time with various time shifts. The right set of curves gives the IM evaluation of the heat flux density as determined with the support of the respective temperature curves. The time response of the temperature sensor induces a first order type of response of the inverse method estimation. But the latter has a time response roughly equal to 2 times τ^+_{TC}. The evaluation of the heat flux density will still be good (within the accuracy

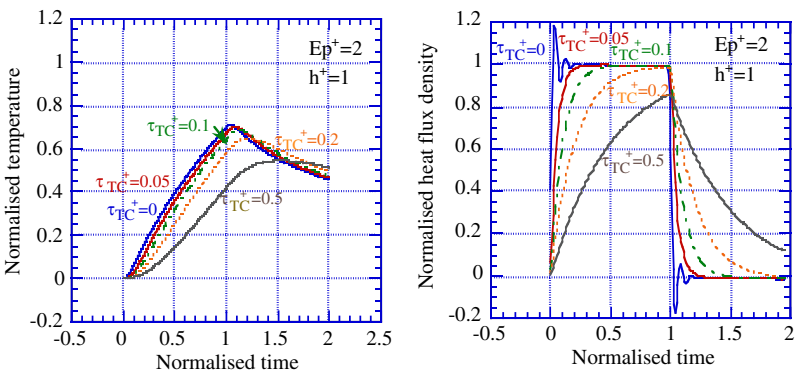

Fig. 8. Impact of time response of the temperature sensor on temperature measurements and on the estimation of the heat flux density on the mating surface, for the strategy point 3 of the map of relevance.

of the map of relevance) if the time response of the thermocouples remains smaller than or equal to 5% of τ. Up to 20% the results are still reasonable in that the magnitude of the heat flux eventually reaches the correct maximum value (nevertheless one can regret some loss of information). A response time larger than 20% of τ would be dramatic in that the maximum value would be underevaluated all the more that the time response is large.

5. Evaluation of thermocouple response time in a HPDC experiment

As stated in the bibliography review, evaluating the actual response-time of temperature sensor in their practical environment (mainly controlled by h_c) is the hardest in transient heat transfer measurements. The normalisation approach that we use enables us to determine it using data from an extremely fast process such as HPDC. The key idea is to use the slopes of the normalised heat flux density curves of Fig. 8 right. They are directly linked to the only τ_{TC} parameter (in the assumption that the heat input is perfectly sudden). Table 3 summarises the relation that appears nearly as an inverse function. This paragraph shows by an example how to do and how consistent the method is.

HPDC is a casting process in which the injection of metal is extremely fast (10–100 ms for several kilograms of aluminium), the pressure applied to the liquid metal is extremely high (10–100 MPa) and the heat transfer is known to be extreme (50–100 kW m^{-2} K^{-1} for the heat transfer coefficient or around 10 MW m^{-2} for the heat flux density [4,6,7,12,49–51]). An innovative 1D device [52] was designed according to our tips and then was used to determine the heat transfer coefficient at the casting/die interface in HPDC. The device measures temperatures with thermocouples in the die at different depth and the surface temperature of the casting with a pyrometer connected to a sapphire crystal in contact to the casting, via an optic fibre. The thermocouples data is used with our standard IM to determine the heat flux density history. Using this as an input in a direct calculation, it possible to re-evaluate the temperatures at any location in the device. One of them is the surface temperature of the die. The three pieces of information about surface temperature of the casting, of the die and the heat flux density at the interface is used to finally determine the interfacial heat transfer coefficient as a function of time.

Table 3
Normalised initial slopes due to sensor response time

Normalised time responses	Normalised initial slopes
0	80 (should be infinite)
5%	16
10%	9
20%	4.5
50%	1.8

The duration of the heat input is the critical parameter that is necessary in order to be able to apply the above principles to the design of a sensor. Direct cavity pressure measurements (using a KISTLER UXE-26510-002 sensor whose response time is 7 μs) were used to estimate it. The assumption was that pressure and heat transfer must be correlated: when the in cavity pressure starts dropping, the contact between the casting and the die impairs and the heat transfer lowers. The duration was found to be about $\tau = 0.5$ s [53]. The decision was taken to use location 3 on the map of relevance. As a direct consequence of this choice, the location of the nearest thermocouple from the interface had to be 1 mm and the data had to be recorded at 200 Hz. The thermocouples were 0.25 mm grounded K-type thermocouples in order to minimise their response time (later estimated to be 40 ms, i.e. 8% of τ). The die was made of H13 steel ($\kappa = 8 \times 10^{-6}$ m^2 s^{-1}).

Fig. 9 gives the results of the IM evaluation of the heat flux density, and the temperatures at three locations (1, 10 and 20 mm) as measured and as re-evaluated from the heat flux density history. The two curves at the top marked with open triangles are related to the surface temperatures of the die and the casting. The top curve, that of the casting surface, was measured with a pyrometer. The second curve, the die surface, was evaluated with a direct heat transfer simulation, knowing the heat flux density on one boundary and the temperature at 20 mm as a second boundary condition. The heat transfer coefficient (h, in black) was evaluated from the derived heat flux density at the interface and the two surface temperatures.

The evaluations of heat flux density and of heat transfer coefficient don't seem to be influenced by any autocorrelation effect that could have been expected with a 200 Hz sampling rate without filtering. The fact is that the measured signal did have an imposed 50 Hz noise component, which resulted in significant autocorrelation in the results sampled at 200 Hz. Nevertheless the standard deviation characterising the noise of our signal was as low as 2.6 °C when the signal was not filtered at all and 2.1 °C when numerically filtered with a FFT band-block filter to remove the 50 Hz noise. This means that most of the noise results from random white noise. However if the contribution of 50 Hz were to be more important, extra care should be taken when choosing ntf so that to avoid interference between the IM and the autocorrelation.

After evaluation, the heat input duration seems to be closer to 0.2 s rather than 0.5 s. This means that our strategic point is no longer point 3 on the map of relevance (see Fig. 5) but point A, however this is still in the acceptable zone.

The time response of the thermocouples is estimated assuming that the initial slope of the heat flux density curve is only related to the effect of the delay due to the thermocouples and that the actual heat input is perfectly sudden (due to the extreme swiftness of the cavity filling stage). In these conditions, the experimental slope can be compared to the simulated slope Fig. 8. The initial experimen-

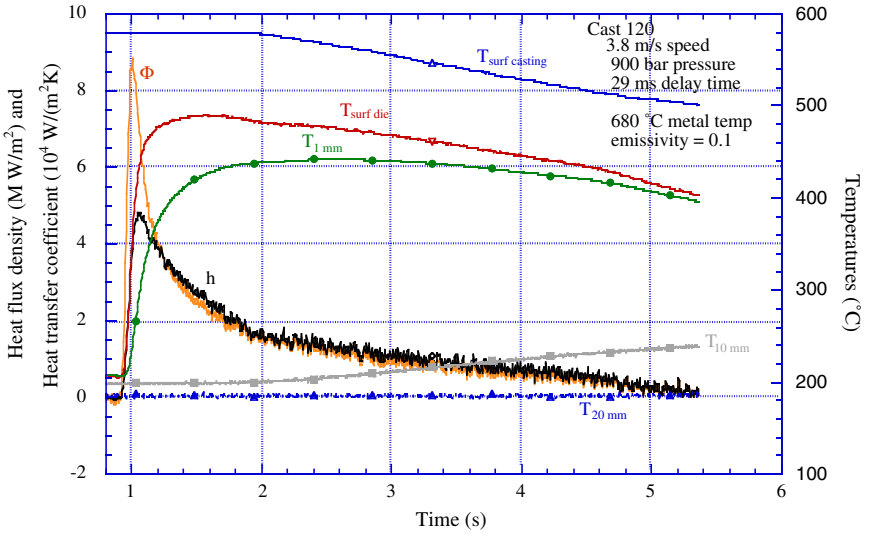

Fig. 9. Result of interfacial heat transfer measurement in HPDC.

tal $d\phi_{exp}/dt$ is about 2×10^8 W m^{-2} s^{-2}. The method used for the comparison is to normalise the experimental slope and compare it to the normalised ones $d\phi^+/dt^+$ reported in Table 3:

$$\frac{d\phi^+}{dt^+} = \frac{d\phi_{exp}}{dt}\frac{\tau}{\phi_{max}} \tag{25}$$

The numerical application in our case ($\tau = 0.2$ s and $\phi_{max} = 8.5$ MW m^{-2}) gives 4.7, which is close to the initial slope for the 20% response time in Table 3. This means that the actual time response of the thermocouples would be in the order of 40 ms. This also means that the peak value of the heat flux density is relevant to the actual heat input. However the precise shape of the heat flux curve in the first 0.2 s is more a reflection of the kinetics of the thermocouples themselves than the true physical phenomenon.

It is noteworthy that the method of determination is self-consistent in the way that the result doesn't depend on the initial choice of τ. If τ had been taken to be twice as large (i.e. 0.4 s), then the result of Eq. (25) would have been 9.4 that compares with 10% of τ. That is to say that the time response of the thermocouple would consistently be 40 ms.

6. Conclusion

A method is proposed in order to perform accurate 1D interfacial heat transfer evaluation using an inverse method. Firstly, a simple procedure is given to evaluate the depth of penetration of thermocouples into the medium to be measured. The result is an over estimation of what would be just necessary, but a closer value is not known yet. A strategy to obtain relevant heat transfer evaluation with an inverse method is described. It is based on the crucial information about the duration of the heat input. A relevant output will be obtained provided that a relation between position of the first thermocouple and the sampling rate is respected, and moreover that the response time of the thermocouple is less than 20% of the heat input duration. The deterministic and stochastic errors to the interfacial heat transfer are explored. Finally the application of the theoretical approach is shown for one extreme condition: interfacial heat transfer in High Pressure Die Casting.

Normalising the heat transfer equation with regard to the heat input duration enables building a map of relevance and to evaluate the deterministic errors of the heat transfer. It also helps determining the time response of the thermocouple once the measurements are performed and checking if the measurements are relevant.

The impact of filtering the temperature data prior to the inverse method evaluations is discussed.

6.1. Note: justification of thermo-physical data from Table 2

The thermocouples are constructed from a core of the two thermocouple element wires, surrounded and separated by electrically insulating MgO powder and contained in a metal sheath. The composite assembly is then mechanically reduced in section to the required diameter. The authors are not aware of the thermocouples having been completely characterised for their thermo-physical properties, and the rationale for the choice of parameters used in this analysis is presented below.

The sheath is made from either Inconel or one of several grades of stainless steel, with room temperature thermal conductivity in the range 10–20 W m^{-1} K^{-1} [33]. We chose 15 W m^{-1} K^{-1}as an average value.

The insulating layer is fine MgO powder, unsintered but relatively well compacted. The degree of compaction was demonstrated in the laboratory when a thermocouple brazed into a piece of steel was sectioned longitudinally and metallographically polished: the powder was not dislodged by any of the grinding or polishing steps. The

thermal conductivity of such a powder depends greatly on the porosity level and particle–particle contacts. An upper limit can be obtained from Touloukian et al. [54] for sintered polycrystalline material at 98% theoretical density, which has a conductivity of 48 $W m^{-1} K^{-1}$ at room temperature, dropping rapidly to 22 $W m^{-1} K^{-1}$ at 300 °C. Slifka et al. [55] reports similar values for sintered material at 93% theoretical density, with slightly lower temperature sensitivity. The Smithells reference book [56] indicates 3.2 $W m^{-1} K^{-1}$. One may argue that sintering would improve the thermal conductivity of a compressed powder. In that uncertain situation we believe the value lies somewhere between 1 and 10 $W m^{-1} K^{-1}$, probably towards the higher end.

The thermocouple wires, Chromel and Alumel, have room temperature conductivities of 19 and 30–32 $W m^{-1} K^{-1}$ respectively [38,57]. Since the wires are of the same diameter, a simple mean should be most accurate, however a value of 32 $W m^{-1} K^{-1}$ was used, which corresponds to the worst case.

The heat transfer coefficients between the MgO and the contacting metal are similarly uncertain. Microscopic examination of the polished section suggest excellent contact, with no detectable gap, and so lower limits are likely to be several thousand $W m^{-2} K^{-1}$.

Acknowledgements

We would like to acknowledge Prof. G. Dunlop for helping to establish the collaboration between our respective institutes and both B. Ladevie and O. Fudym for their initial help in using inverse methods and simulation in heat transfer. We also would like to acknowledge Ferra Engineering Pty. Ltd. and the financial support of the Cooperative Research Centre for Cast Metals Manufacturing (CAST). CAST was established and is funded in part by the Australian Government's Cooperative Research Centres Program. This work was performed during the sabbatical stay of G. Dour in CAST at the University of Queensland. The Ecole des Mines d'Albi-Carmaux and the French Ministry of Economy, Finances and Industry are acknowledged for giving him this opportunity.

References

[1] S. Broucaret, A. Michrafy, G. Dour, Heat transfer and thermomechanical stresses in a gravity die—influence of process parameters, J. Mater. Process. Technol. 110 (2001) 211–217.
[2] W.D. Griffiths, The heat transfer coefficient during the unidirectional solidification of an Al–Si alloy casting, Metall. Mater. Trans. B 30B (1999) 473–482.
[3] C.P. Hallam, W.D. Griffiths, N.D. Butler, Interfacial heat transfer between a solidifying aluminium alloy and a coated die steel, Mater. Sci. Forum 329 (330) (2000) 467–472.
[4] P. Schmidt, Heat Transfer in Permanent Mould Casting, Royal Institute of Technology, Stockholm, 1994.
[5] G. Sciama, J.F. Ribou, Solidification de barreaux en AlSi7Mg coulés contre refroidisseurs, Fondeur Fonderie d'Aujourd'hui 169 (1997) 23–61.
[6] V. Davies, Heat transfer in gravity die castings, Brit. Foundryman 73 (12) (1980) 331–334.
[7] S. Hong, D.G. Backman, R. Mehrabian, Heat transfer coefficient in aluminium alloy die casting, Metall. Trans. B 10B (2) (1979) 299–301.
[8] J.H. Hattel, P.N. Hansen, A 1-D analytical model for the thermally induced stresses in the mold surface during die casting, Appl. Math. Modell. 18 (10) (1994) 550–559.
[9] G.W. Liu, Y.S. Morsi, J.P. VanDerWalt, Analysis of spray cooling heat flux, J. Heat Transfer-Trans. ASME 121 (3) (1999) 742–745.
[10] H. Hu, A. Yu, Numerical simulation of squeeze cast magnesium alloy AZ91D, Modell. Simulat. Mater. Sci. Eng. 10 (1) (2002) 1–11.
[11] J.H. Hu, E.R.G. Eckert, R.J. Goldstein, Numerical simulation of flows, heat transfer and solidification in pressure die casting, in: 28th National Heat Transfer Conference and Exhibition, San Diego, CA, USA, ASME, New York, NY, USA, , 1992.
[12] A. Nahed et al., On the influence of process variables on the thermal conditions and properties of high pressure die-cast magnesium alloys, J. Mater. Process. Technol. 73 (1998) 125–138.
[13] A. Inoue, K. Onoue, T. Masumoto, Microstructure and properties of bulky Al sub 8 sub 4Ni sub 1 sub 0Ce sub 6 alloys with amorphous surface layer prepared by high-pressure die casting, Mater.-Trans. JIM 35 (11) (1994) 808–813.
[14] Konovalov II et al., Bulk amorphous plate production by a casting process, J. Non-Cryst. Solids (1996) 536–539.
[15] L. Strezov, J. Herbertson, G.R. Belton, Mechanisms of initial melt/substrate heat transfer pertinent to strip casting, Metall. Mater. Trans. B 31B (2000) 1023–1045.
[16] N. Ebrill, Y. Durandet, L. Strezov, Dynamic reactive wetting and its role in hot dip coating of steel sheet with an Al–Zn–Si alloy, Metall. Mater. Trans. B 31B (2000) 1069–1079.
[17] T. Evans, L. Strezov, Interfacial heat transfer and nucleation of steel on metallic substrates, Metall. Mater. Trans. B 31B (2000) 1081–1089.
[18] R.I.L. Guthrie et al., Measurements, simulations and analyses of instantaneous heat fluxes from solidifying steels to the surfaces of twin roll casters and of aluminium to plasma-coated metal substrates, Metall. Mater. Trans. B 31B (2000) 1031–1046.
[19] D. Bouchard et al., Effects of substrate surface conditions on heat transfer and shell morphology in the solidification of a copper alloy, Metall. Mater. Trans. B 32B (2000) 111–118.
[20] D. Fraser, M.Z. Jahedi, Die lubrication in high pressure die casting, in: Die Casting and Toolmaking Technology, Melbourne, 1997.
[21] G. Diaconu, G. Dour. Heat transfer and thermal stresses in a centrifugal casting die, in: Fourth International Congress on Thermal Stresses, Thermal Stresses, Osaka, 2001.
[22] M. Bellet et al., Metall. Mater. Trans. B 27B (1996) 81–100.
[23] Z.H. Lee, T.G. Kim, Y.S. Choi, The movement of the concave casting surface during mushy-type solidification and its effect on the heat transfer coefficient, Metall. Mater. Trans. B 29B (1998) 1051–1056.
[24] O. Fudym et al., Heat flux determination in thin-layer drying, in: Proceedings of the Third International Conference on Inverse Problem in Engineering, Port Ludlow, WA, 1999.
[25] D. Maillet et al., Thermal Quadrupoles—Solving the Heat Equation through Integral Transforms, John Wiley, 2000.
[26] J.V. Beck, H. Hurwicz, Effect of thermocouple cavity on heat sink temperature, J. Heat Transfer 82 (1960) 27–36.
[27] N.R. Keltner, J.V. Beck, Surface temperature errors, J. Heat Transfer 105 (1983) 312–318.
[28] M.H. Attia, A. Cameron, L. Kops, Distortion in thermal field around inserted thermocouples in experimental interfacial studies, Part 4: End effect, J. Manuf. Sci. Eng. 124 (2002) 135–145.
[29] J.P. Bardon, Mesure de température et de flux de chaleur par des méthodes par contact, in: Ecole d'Hiver—METTI'99, Odeillo, 1999.
[30] J.P. Bardon, M. Raynaud, Y. Scudeller, Mesure par contact des temperatures de surface, Rev. Gén. Therm. 34 (1995) 15–35.
[31] D. Li, M. Wells, Effect of sub-surface thermocouple installation on the error of the measured thermal history and predicted surface heat flux during a quench operation. Metall. Mater. Trans. B, in press.

[32] K.A. Woodbury, Effect of thermocouple sensor dynamics on surface heat flux predictions obtained via inverse heat transfer analysis, Int. J. Heat Mass Transfer 33 (12) (1990) 2641–2649.
[33] Milano G. Some strategy for handling measurements biases in inverse problems with application thermal properties identification, in: Ecole d'Hiver—METTI, Odeillo, France, 1999.
[34] W.M. Rohsenow, J.P. Hartnett, E.N. Ganic (Eds.), Handbook of Heat Transfer Applications, second ed., McGraw-Hill, 1985.
[35] Thermocoax, Quel thermocouple choisir? 2002, Thermocoax S.A.: Lyon, pp. 2–31.
[36] Omega, The Temperature Handbook, Omega Ldt., 2002.
[37] J.V. Beck, B. Blackwell, A. Haji-Sheikh, Comparison of some inverse heat conduction methods using experimental data, Int. J. Heat Mass Transfer 39 (17) (1996) 3649–3657.
[38] M. Raynaud, Détermination du flux surfacique traversant une paroi à partir de mesures de températures internes, Université de Paris VI, Paris, 1984.
[39] E. Hensel, R.G. Hills, An initial value approach to the inverse heat conduction problem, Trans. ASME, J. Heat Transfer 108 (1986) 248–256.
[40] A.F. Emery, T.D. Fadale, Design of experiments using uncertainty information, Trans. ASME, J. Heat Transfer 118 (1996) 532–538.
[41] T.D. Fadale, A.V. Nenarokomov, A.F. Emery, Two approaches to optimal sensor locations, Trans. ASME, J. Heat Transfer 117 (1995) 373–379.
[42] A.F. Emery, T.D. Fadale, The effect of imprecisions in thermal sensor location and boundary conditions on optimal sensor location and experimental accuracy, J. Heat Transfer 119 (1997) 661–665.
[43] G.P. Flach, M.N. Özisik, Inverse heat conduction problem of periodically contacting surfaces, J. Heat Transfer 110 (1988) 821–829.
[44] J.P. Holman, Heat Transfer, seventh ed., McGraw-Hill, 1990.
[45] M.H. Attia, L. Kops, Distortion in thermal field around inserted thermocouples in experimental interfacial studies—Part II: Effect of the heat flow through the thermocouple, J. Eng. Indus. 110 (1988) 7–14.
[46] B.S. Singh, A. Dybbs, Errors in temperature measurements due to conduction along the sensor leads, ASME J. Heat Transfer (1976) 491–495.
[47] J. Taine, J.P. Petit, Transferts Thermiques, Dunod, 1995.
[48] D. Couedel, Etude des transferts thermiques lors de la mise en contact périodique de deux milieux solides—application au système soupape-siège dans un moteur à combustion interne, in: ISITEM. 1002, Université de Nantes, Nantes.
[49] G. Dour, Thermal stresses and distortion in dies of die casting processes—a new normalised approach, Modell. Simulat. Mater. Sci. Eng. 9 (2001) 399–413.
[50] Y. Hatamura et al., Direct measurement of metal pressure and die surface temperature, in: World of Die Casting: 1989, North American Die Casting Association, 1989.
[51] J. Papai, C. Mobley, Die thermal fields and heat fluxes during die casting of 380 aluminium alloy in H13 steel dies, in: World of Die Casting: 1991, North American Die Casting Association, 1991.
[52] G. Dour, M. Dargusch, C. Davidson, Developments relating to measurements of temperatures and heat transfer coefficients, in: Patent application no. 20029553328, Australia, 2002.
[53] G. Dour et al., Development of a non-intrusive heat transfer coefficient gauge and its application to high pressure die casting, in: Light Metals Technology, Brisbane, 2003.
[54] Y.S. Touloukian, P.E. Liley, S.C. Saxena, Thermal Conductivity. Non-metallic Solids, IFI/Plenum, New York, 1970.
[55] A.J. Slifka, B.J. Filla, J.M. Phelps, J. Res. Natl. Inst. Stand. Technol. 103 (1998) 357.
[56] C.J. Smithells, Smithells Metals Reference Book, seventh ed., Butterworth–Heinemann, 1992.
[57] GoodfellowSARL, http://www.goodfellow.com, données techniques, T2, Alliage pour thermocouples Ni95/(Al+Mn+Si) 5, 2004.
[58] M.N. Özisik, Heat Conduction, John Wiley, 1993.
[59] B. Bourouga, V. Goizet, J.P. Bardon, Les aspects théoriques régissant l'instrumentation d'un capteur thermique parietal à faible inertie, Int. J. Therm. Sci. 39 (2000) 96–109.